Photoluminescence Properties of the Structurally Analogous Tetranuclear Copper(I) Clusters $Cu_4X_4(dpmp)_4$ (X = I, Br, Cl; dpmp = 2-(Diphenylmethyl)pyridine)

Chong Kul Ryu, Marcello Vitale, and Peter C. Ford*

Department of Chemistry, University of California, Santa Barbara, California 93106

Received July 22, 1992

Reported are the photophysical properties of the copper(I) halide clusters $Cu_4X_4(dpmp)_4$ with the bulky organic base 2-(diphenylmethyl)pyridine (X = I, Br, Cl) which have been shown by previous crystal structure determinations to have "cubane"-like Cu_4X_4 cores with very similar Cu–Cu distances (2.87–3.01 Å). As solids at 77 K, these compounds each exhibit a strong, relatively long-lived emission band [λ_{max}^{em} = 467, 487, and 505 nm; τ = 18.1, 10.0, and 10.0 μs (for X = I, Br, and Cl, respectively)], which is attributed to radiative decay from a halide to ligand charge transfer (XLCT) excited state. At higher temperatures, a weak shoulder appeared in the emission spectra for the $Cu_4I_4(dpmp)_4$ and $Cu_4Br_4(dpmp)_4$ solids (at ~570 and ~626 nm, respectively), and the relative intensities of these shoulders could be fit to the function $A\exp(-\Delta E/RT)$, with ΔE = 990 ± 370 cm^{-1} for the appearance of this red emission in $Cu_4Br_4(dpmp)_4$. The excited state (ES) lifetimes observed for these shoulders were identical to those observed for the still dominant higher energy bands. In analogy to earlier results with the copper(I) iodide cluster $Cu_4I_4(py)_4$, this longer wavelength band was attributed to emission from a Cu_4X_4 core centered ES of mixed halide-to-copper charge transfer (XMCT) and metal centered "d–s" orbital parentage. The nature of such transitions in $Cu_4X_4L_4$ clusters is discussed with respect to the Cu–Cu distances in the ground state structures.

Introduction

Studies in this laboratory[1-3] and others[4-8] have demonstrated the remarkably rich luminescence behavior of the "cubane"-like tetranuclear cuprous halide clusters $Cu_4X_4L_4$ (X = Cl, Br, I; L = a nitrogen or phosphine organic base) (Figure 1). The most extensively probed member of this series is $Cu_4I_4(py)_4$ (A, py = pyridine), which displays two independent emissions, the apparent result of very poor coupling between the relevant excited states (ES).[1,2] In ambient toluene solution, these were evident as a weak, higher energy (HE) band with λ_{max}^{em} = 480 nm, τ = 450 ns and a more intense, lower energy (LE) emission with λ_{max}^{em} = 690 nm, τ = 10.6 μs.[2] Similar emission properties are displayed by other $Cu_4I_4L_4$ clusters, but the HE band has been seen only for those clusters having π-unsaturated L's.[3] As a consequence, the HE emission was first assigned as being from a metal-to-ligand charge transfer (MLCT) ES,[1] but ab initio calculations have since concluded that the relevant ES must be largely halide-to-pyridine charge transfer (XLCT) instead.[1c,2,9] In contrast, the LE band has been observed in the emission spectra of $Cu_4I_4L_4$ clusters having either aromatic and saturated amine L's and the relevant ES assigned as "cluster centered" (CC), a mixture of iodide-to-copper charge transfer (XMCT) and metal centered "d-to-s" (MC) in orbital parentage.[1c,2,9] The poor coupling between these ES can be attributed to the much greater distortion of the CC state.[2,9]

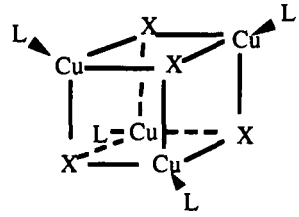

Figure 1. "Cubane"-type structure of the $Cu_4X_4L_4$ clusters where L is a nitrogen or phosphorus organic base and X is a halide. For I, II and III, L = 2-($CHPh_2$)py (dpmp) and X = I, Br and Cl, respectively.

Of particular interest is the role of metal-metal interactions in the relevant excited states of these and related d^{10} metal ion clusters,[10-12] especially the CC state, since the filled, highest energy d-orbitals are formally antibonding while the empty s-orbitals are bonding with respect to the copper–copper interactions within the cluster core. Since both the XMCT and MC components of

(1) (a) Kyle, K. R.; DiBenedetto, J.; Ford, P. C. *J. Chem. Soc., Chem. Commun.* **1989**, 714–715. (b) Kyle, K. R.; Ford, P. C. *J. Am. Chem. Soc.* **1989**, *111*, 5005–5006. (c) Kyle, K. R.; Palke, W. E.; Ford, P. C. *Coord. Chem. Rev.* **1990**, *97*, 35–46.
(2) Kyle, K. R.; Ryu, C. K.; Ford, P. C. *J. Am. Chem. Soc.* **1991**, *113*, 2954–2965.
(3) Ryu, C. K.; Kyle, K. R.; Ford, P. C. *Inorg. Chem.* **1991**, *30*, 3982–3986.
(4) (a) Hardt, H. D.; Pierre, A. *Inorg. Chim. Acta* **1977**, *25*, L59–L60 and references therein. (b) Hardt, H. D.; Stroll, H.-J. *Z. Anorg. Allg. Chem.* **1981**, *480*, 193–198. (c) Hardt, H. D.; Stroll, H.-J. *Z. Anorg. Allg. Chem.* **1981**, *480*, 199–204.
(5) (a) Radjaipour, M.; Oelkrug, D. *Ber. Bunsen-Ges. Phys. Chem.* **1978**, *82*, 159–163. (b) Eitel, E.; Oelkrug, D.; Hiller, W.; Strähle, J. *Z. Naturforsch.* **1980**, *35B*, 1247–1253.
(6) Vogler, A.; Kunkely, H. *J. Am. Chem. Soc.* **1986**, *108*, 7211–7212.
(7) (a) Rath, N. P.; Holt, E. M.; Tanimura, K. *Inorg. Chem.* **1985**, *24*, 3934–3938. (b) Rath, N. P.; Holt, E. M.; Tanimura, K. *J. Chem. Soc., Dalton Trans.* **1986**, 2303–2310.
(8) Henary, M.; Zink, J. I. *J. Am. Chem. Soc.* **1989**, *111*, 7404–7411.
(9) Vitale, M.; Palke, W. E.; Ford, P. C. *J. Phys. Chem.* **1992**, *96*, 8329–8336.
(10) Sabin, F.; Ryu, C. K.; Vogler, A.; Ford, P. C. *Inorg. Chem.* **1992**, *31*, 1941–1945.
(11) Kutal, C. *Coord. Chem. Rev.* **1990**, *99*, 213–252.
(12) (a) Stillman, M. J.; Zelazowski, A. J.; Szymanska, J.; Gasyma, Z. *Inorg. Chim. Acta* **1989**, *161*, 275–279. (b) Vogler, A.; Kunkely, H. *Chem. Phys. Lett.* **1989**, *158*, 74–76. (c) Vogler, A.; Kunkely, H. *Chem. Phys. Lett.* **1988**, *150*, 135–137. (d) King, C.; Wang, J.-C.; Khan, M. N. I.; Fackler, J. P. *Inorg. Chem.* **1989**, *28*, 2145–2149. (e) Kahn, M. N. I.; Fackler, J. P.; King, C.; Wang, J. C.; Wang, S. *Inorg. Chem.* **1988**, *27*, 1672–1673. (f) Che, C.-M.; Wong, W.-T.; Lei, T.-F.; Kwong, H.-L. *J. Chem. Soc., Chem. Commun.* **1989**, 243–244. (g) Che, C.-M.; Kwon, H.-L.; Yam, V. W.-W.; Cho, K.-C. *J. Chem. Soc., Chem. Commun.* **1989**, 885–886. (h) Balch, A. C.; Catalano, V. J.; Olmstead, M. M. *Inorg. Chem.* **1990**, *29*, 585–586. (i) Perreault, D.; Drouin, M.; Michel, A.; Harvey, P. D. *Inorg. Chem.* **1991**, *30*, 2–4. (j) Assefa, Z.; Destefano, F.; Garepapaghi, M. A.; LaCasce, J. H., Jr.; Ouellete, S.; Corson, M. R.; Nagle, J. K.; Patterson, H. H. *Inorg. Chem.* **1991**, *30*, 2868–2876. (k) McCleskey, T. M.; Gray, H. B. *Inorg. Chem.* **1992**, *31*, 1733–1734. (l) Kunkely, H.; Vogler, A. *Chem. Phys. Lett.* **1989**, *164*, 621–624. (m) Kane-Maguire, N. A. P.; Wright, L. L.; Guckert, J. A.; Tweet, W. S. *Inorg. Chem.* **1988**, *27*, 2905–2907. (n) Harvey, P. D.; Schaefer, W. P.; Gray, H. B. *Inorg. Chem.* **1988**, *27*, 1101–1104. (o) Harvey, P. D.; Gray, H. B. *J. Am. Chem. Soc.* **1988**, *110*, 2145–2147. (p) Harvey, P. D.; Dallinger, R. F.; Woodruff, W. H.; Gray, H. B. *Inorg. Chem.* **1989**, *28*, 3057–3059. (q) Henary, M.; Zink, J. I. *Inorg. Chem.* **1991**, *30*, 3111–3112.

0020-1669/93/1332-0869$04.00/0

a CC transition involve populations of the s-orbitals, this ES should display enhanced metal–metal bonding within the Cu_4 core and structural distortions consistent with the very large Stokes shifts observed for the CC emission. Notable in this context is the observation by Holt[7] that CC emissions are found only for those clusters with Cu–Cu distances (d_{Cu-Cu}) less than twice the van der Waals radius of Cu(I) (1.4 Å). Consistent with this suggestion, a CC band is seen[2,6] for $Cu_4I_4(pip)_4$ (B, pip = the saturated amine piperidine) with d_{Cu-Cu} = 2.65 Å but not[3] for $Cu_4Cl_4(Et_3N)_4$ (C, Et_3N = triethylamine) with d_{Cu-Cu} = 3.07 Å.

These two examples (B and C) illustrate a major problem in evaluating proposed assignments of the d^{10} cluster photophysical properties. Given the ab initio calculations[1c,9] which point to the predominant contribution of the halide orbitals to the cluster HOMO's, it would be especially desirable to consider carefully the photophysical properties of $Cu_4X_4L_4$ clusters for which the effect of changing the halide is not accompanied by corresponding major variations in the molecular and crystal structures. This indeed is the case for the homologous series of the clusters $Cu_4X_4(dpmp)_4$ where dpmp is the very bulky organic ligand 2-(diphenylmethyl)pyridine and X is Cl, Br or I. The crystal structures of these compounds have been determined[13] and shown to be isomorphous and isostructural in the tetragonal space group $I4_1/a$. For each of these clusters the Cu_4 tetrahedra are nearly identical and display an average d_{Cu-Cu} ~2.90 Å. Described here are the photophysical properties of these complexes.

Experimental Section

Materials. Acetonitrile (AN) and methanol were distilled over CaH_2 under N_2 atmosphere. Toluene was dried and distilled over Na metal under N_2. Cuprous halides (CuI, CuBr and CuCl) were purified by the literature methods.[14,15] 2-(Diphenylmethyl)pyridine (dpmp, 99%, Aldrich) was used as received. Potassium iodide and $MgCO_3$ (Fisher) were also used as received.

The $Cu_4I_4(dpmp)_4$ (I), $Cu_4Br_4(dpmp)_4$ (II) and $Cu_4Cl_4(dpmp)_4$ (III) clusters were prepared by the published methods.[13] All syntheses and manipulation of the solutions were performed under argon atmosphere with modified Schlenk techniques. All samples were checked via X-ray powder diffraction analyses of solids and the X-ray powder diffraction pattern, and intensity profiles were shown to match well with those derived from the single crystal cell parameters.[13]

Physical Measurements. High resolution powder diffraction data were collected for each sample by a Scintag Pad X automated X-ray diffractometer by using Cu Kα radiation.

The UV–visible spectra were recorded on a HP 8452 diode array spectrophotometer. Diffuse reflectance (DR) spectra were recorded on a Cary 14 UV–vis spectrophotometer equipped with an integrating sphere and an On-Line Instrument Systems (OLIS) computer controller in the laboratory of Professor G. Stucky at UCSB. Solid $MgCO_3$ was used as reference for the DR spectra.

The steady state emission and excitation spectra were recorded on the Spex Fluorolog 2 spectrofluorimeter with a cooled Hamamatsu R928 photomultiplier as described elsewhere.[2] The emission lifetimes were determined at 298 and 77 K by using the Quanta Ray DCR-1A Q-switched Nd:YAG laser system and RCA 8852 or EMI 9816A photomultiplier tube (PMT) and techniques described previously.[2] Variable temperature emission spectral measurements were made of solid samples in Pyrex capillary tubes in a Pyrex dewar with appropriate cooling bath: 273 K (ice/H_2O), 250 K (CO_2/CCl_4), 218 K and 203 K (CO_2/MeOH), 143 K (*n*-pentane/liquid N_2), 77 K (liquid N_2). The temperature of the cooling bath was checked with a thermometer or thermocouple each time.

Electrochemical Measurements. Cyclic voltammetric measurements were carried out by using a Bioanalytical System Model 100 A electrochemical analyzer in the laboratory of Professor W. C. Kaska at UCSB. The AN solution contained 0.1 M tetra-*n*-butylammonium hexafluorophosphate (TBAH) as supporting electrolyte. $E_{1/2}$ values, determined as $(E_{pa} + E_{pc})/2$, were referenced to the Ag/AgCl electrode with scan rate 100 mV/s. A Pt- or an Au-disk working electrode and a Pt wire auxiliary electrode were also employed in these electrochemical measurements.

Table I. Electronic Absorption and Diffuse Reflectance Spectral Data for $Cu_4X_4(dpmp)_4$ at 298 K

compound	λ_{max}^{ab} (nm) (10^{-3} ϵ (M^{-1} cm^{-1}))[a]	λ_{max}^{dr} (nm)[b]
$Cu_4I_4(dpmp)_4$	270 (sh, 13.4), 248 (59.0)	~266, 371
$Cu_4Br_4(dpmp)_4$	270 (sh, 11.3), 260 (16.4)	~266, 368
$Cu_4Cl_4(dpmp)_4$	270 (sh, 12.1), 260 (16.7)	266, 368
dpmp[c]	270 (sh, 2.96), 260 (4.05)	
KI	248 (12.8)	

[a] Absorption maxima in acetonitrile. sh = shoulder. [b] Diffuse reflectance maxima in solids. [c] λ_{max}^{ab} = 272 and 263 nm in CH_3OH (*Sadtler Standard Spectra*; Sadtler Research Laboratories: Philadelphia, PA, 1975–1978).

Results

Electronic Absorption Spectra. Table I lists the spectral data for the $Cu_4X_4(dpmp)_4$ clusters, free ligand dpmp and KI in AN solution at room temperature. The λ_{max}^{ab} of II and III at 260 and 270 (sh) nm are the same as the π–π^* maxima of the free ligand dpmp in the same medium with molar extinction coefficients (ϵ_{max}) ~4-fold higher, consistent with the presence of four dpmp ligands in each cluster. The spectrum of the iodide analog, I, in AN solution displays an intense band at λ_{max}^{ab} = 248 nm (ϵ = 5.90×10^4 M^{-1} cm^{-1}) and a shoulder at 270 nm (1.34×10^4 M^{-1} cm^{-1}). The former band is close to that observed for KI in AN solution with ϵ_{max} ~4-fold higher, as expected. The only absorption spectra features unique to the clusters are longer wavelength shoulders which tail to 400 nm. For the wavelengths 340 and 370 nm (chosen because of their correspondence to features in the diffuse reflectance and/or excitation spectra, see below) these absorptions have ϵ values of 278 and 67 M^{-1} cm^{-1}, 227 and 72 M^{-1} cm^{-1} and 120 and 37 M^{-1} cm^{-1} for I, II and III, respectively. Notably, absorptions in this region gave linear Beer's law plots over the concentration range 10^{-4} to 6×10^{-3} M for all three compounds in AN solutions, indicating that the clusters remain intact at these concentrations.[16] Absorptions at $\lambda > 300$ nm are not seen in the spectra of KI, dpmp or $[Cu(AN)_4]BF_4$ individually in AN solution at comparable concentrations.

Diffuse Reflectance Spectra. Table I also lists the DR maxima of the respective $Cu_4X_4(dpmp)_4$ solids at room temperature. Each of these DR spectra exhibits two broad bands, one centered at 260–270 nm and the other at ~370 nm (Figure 2), although the brighter emitters (I and II) displayed some interference for the higher energy band due to apparent "negative reflectance" in the short wavelength region. (In order to reduce this, the samples were diluted with $MgCO_3$ ca. 1 to 5% samples by weight). The higher energy band obviously corresponds to the ligand centered absorptions at 260 and 270 nm while the longer wavelength feature agrees with the longer wavelength tail seen in solution absorption.

Emission Spectra. The luminescence properties of the respective $Cu_4X_4(dpmp)_4$ solids are summarized in Table II. At 77 K, these exhibited relatively intense and narrow bands ($\Delta\nu_{1/2}$ ~ 3200 cm^{-1}) at λ_{max}^{em} = 467 (446 (sh)), 487 and 505 nm for X = I, Br and Cl, respectively (Figure 3). Some structure is noted in the spectrum of I with a spacing of ~1100 cm^{-1}.

At 298 K, the emission spectra of the three $Cu_4X_4(dpmp)_4$ solids exhibited a strong band analogous to those seen at lower *T*, λ_{max}^{em} = 440 and 462 (sh) for I, 480 nm for II and 500 nm for III (Figure 4). Each of these bands was somewhat broadened to longer wavelengths; indeed a new feature, a weak shoulder,

(13) Engelhardt, L. M.; Healy, P. C.; Kildea, J. D.; White, A. H. *Aust. J. Chem.* **1989**, *42*, 107–113.
(14) Kauffmann, G. B.; Fang, L. Y. *Inorg. Synth.* **1983**, *22*, 101–103.
(15) Keller, R. N.; Wycoff, H. D. *Inorg. Synth.* **1946**, *2*, 1–4.

(16) Good Beer's law plots were observed at shorter λ for all three clusters in the 10^{-6} to 10^{-4} M region. However, the similarity of free ligand and cluster spectra in this region makes it impossible to preclude ligand dissociation or even complete disassembling of the cluster. Notably, similar solutions rapidly quenched in liquid N_2 to give glassy solutions are still luminescent, a characteristic cluster property.

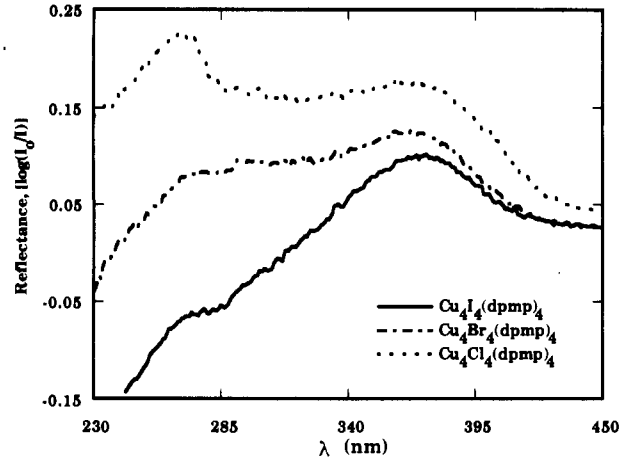

Figure 2. Diffuse reflectance spectra of solid $Cu_4X_4(dpmp)_4$ vs $MgCO_3$ at 298 K.

Table II. Photophysical Properties of $Cu_4X_4(dpmp)_4$ as Solids

T (K)	λ_{max}^{em} (nm)[a]	$\Delta\nu_{1/2}$ (10^3 cm^{-1})[b]	λ_{max}^{ex} (nm)[c]	ΔE (10^3 cm^{-1})[d]	τ (μs)[e]
		X = I			
77	446 (sh),[f] 467	3.4	333 (sh), 360, 372 (sh)	6.4	18.1
298	440, 462 (sh) 570 (sh)		370 (br)	4.3 9.5	7.5
		X = Br			
77	487	3.3	327 (sh), 357, 374 (sh)	7.5	10.0
298	480, ~626 (sh)		360 (br)	6.9 11.8	0.54
		X = Cl			
77	505	3.0	330 (sh), 366, 383 (sh)	7.5	10.0
298	500		360 (br)	7.8	2.7

[a] Emission maxima. [b] Full width at half-maximum. [c] Excitation maxima. [d] $\Delta E = \nu_{max}^{ex} - \nu_{max}^{em}$. [e] Measured lifetime. [f] sh = shoulder; br = broad.

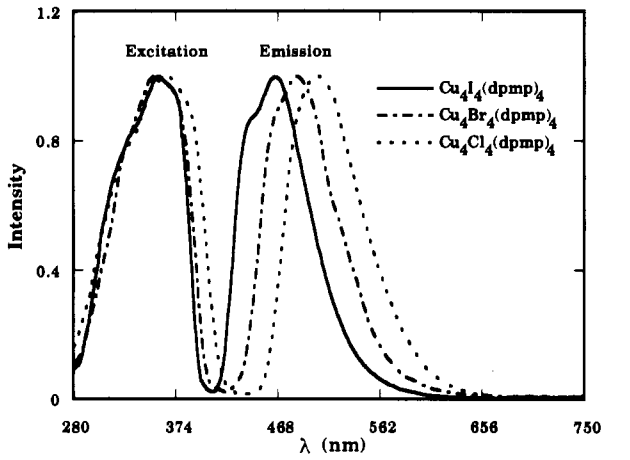

Figure 3. Excitation and emission spectra of solid $Cu_4X_4(dpmp)_4$ at 77 K.

was observed in the emission spectrum of I (~570 nm) and that of II (~626 nm).

The emission spectrum (λ^{ex} = 380 nm) of solid $Cu_4Br_4(dpmp)_4$ displayed the dependence on temperature (77–295 K) indicated in Figure 5 with spectral intensities at ~480 nm normalized to 1. At 77 K, only one emission band (λ_{max}^{em} = 487 nm) was apparent, but a second emission band at ~626 nm became evident at 203 K and continued to grow in relative intensity with increasing T. The ratios R of the integrated areas of the two bands were determined from a Gaussian analysis of the band shapes, and a

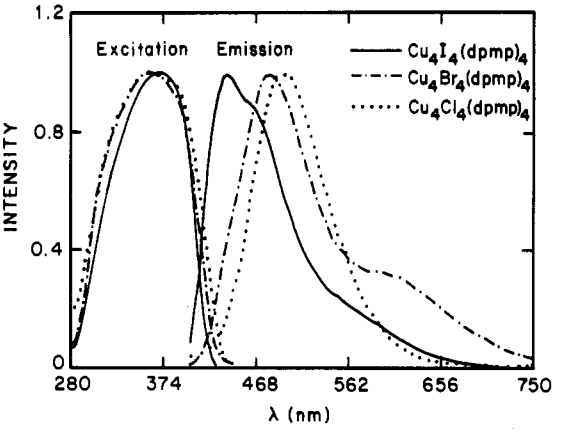

Figure 4. Excitation and emission spectra of solid $Cu_4X_4(dpmp)_4$ at 298 K.

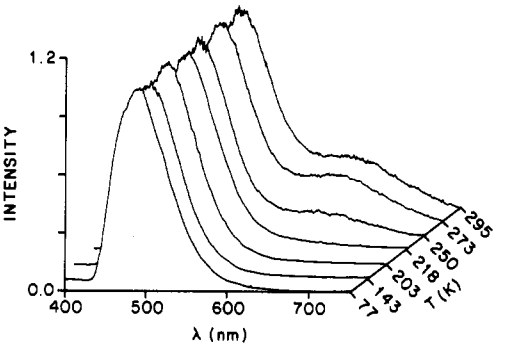

Figure 5. Temperature dependence of emission spectra of solid $Cu_4Br_4(dpmp)_4$ with 380 nm excitation.

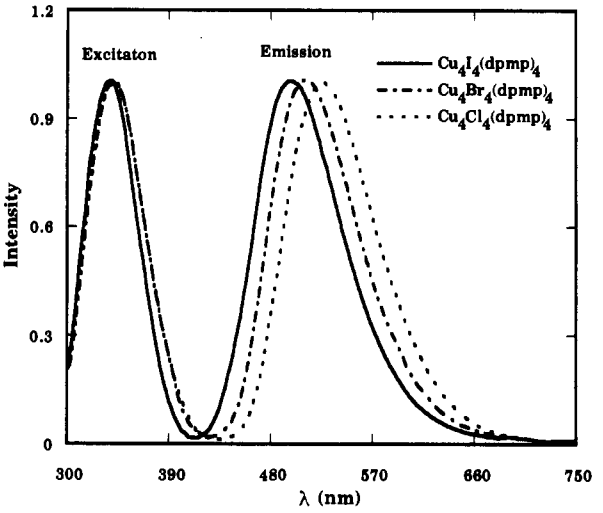

Figure 6. Excitation and emission spectra of $Cu_4X_4(dpmp)_4$ in AN at 77 K. [I] = 0.12 mM, [II] = 0.11 mM, and [III] = 0.10 mM.

numerical fit of $R = A\exp(-\Delta E/RT)$ gave a value of 990 ± 370 cm^{-1} for ΔE for the appearance of the red emission. A similar result was obtained with 320 nm excitation.

Frozen AN solutions (77 K) of I, II and III at various concentrations (10^{-3}–10^{-5} M) exhibited broad emission bands with similar band shapes and widths ($\Delta\nu_{1/2}$ ~ 3400 cm^{-1}) (Figure 6) and with λ_{max}^{em} at 500, 512 and 530 nm, respectively (Table III), red-shifted about 25–30 nm from those seen for the respective solids at 77 K. The shapes and positions of these bands proved to be independent of sample concentration over a 10^{-3}–10^{-5} M range. The emission spectra in 77 K toluene glassy solutions were very similar and displayed bands at 501, 496 and 530 nm, respectively. Emission was not detected from AN or toluene solutions of any of the $Cu_4X_4(dpmp)_4$ clusters at ambient temperature.

Table III. Photophysical Properties of AN Solutions of $Cu_4X_4(dpmp)_4$ Clusters at 77 K

X	λ_{max}^{em} (nm)[a]	$\Delta\nu_{1/2}$ (10^3 cm^{-1})[b]	λ_{max}^{ex} (nm)[c]	λ_{max}^{ex} (nm)[d]	ΔE (10^3 cm^{-1})[e]	τ (μs)
I	500	3.4	339	350, 380[f]	6.3	15.3
Br	512	3.4	341	355, 380[f]	6.8	12.5
Cl	530	3.3	341	354, 380[f]	7.4	12.8

[a] Emission maximum. [b] Full width at half-maxima. [c] Excitation maximum at low concentration. [d] Excitation maxima at high concentration. [e] $\Delta E = \nu_{max}^{ex} - \nu_{max}^{em}$. [f] Shoulder.

The emission spectra of all three $Cu_4X_4(dpmp)_4$ clusters as solids or in frozen AN solutions proved to be independent of λ^{ex} from 320 to 380 nm.

Excitation Spectra. The excitation spectra of the respective $Cu_4X_4(dpmp)_4$ solids were obtained by monitoring at the respective emission maxima. These data are summarized in Table II.

At room temperature, the excitation spectra of solid I, II and III each displayed a broad band centered at ~365 nm (Figure 4). The spectra were differentiated only by small edge effects in the energy order I > II > III but were independent of whether the emission was monitored at λ_{max}^{em} or at the longer wavelength tail. Thus, in each case, these emissions apparently originate from a common excited state or several equilibrated ES, and the possible intervention of impurities as the origin of the emission tail can be ruled out. There was some overlap between the respective excitation and emission spectra.

At 77 K, the excitation spectra of solid I, II and III displayed relatively narrow but similar maxima at λ_{max}^{ex} ~ 365 nm (shoulders at ~330 and ~375 nm) along with a edge effect similar to that observed at room temperature (Figure 4). However, there was less overlap between excitation and emission spectrum of each $Cu_4X_4(dpmp)_4$ than seen at room temperature (Figures 3 and 4).

In frozen AN solution, the excitation spectra of the respective $Cu_4X_4(dpmp)_4$ clusters were measured both at concentrations $\leq 10^{-4}$ M and ~10^{-3} M while monitoring the respective λ_{max}^{em}. At the lower concentration, each compound displayed an excitation band at λ_{max}^{ex} ~ 340 nm (Table III) which was narrower and displayed less edge effect than for the solid at 77 K. However, at the higher concentration, homogeneous solutions of each $Cu_4X_4(dpmp)_4$ displayed a λ_{max}^{ex} at ~350 nm plus a shoulder at ~380 nm, features closer to those observed for the solid state. The excitation spectra of I, II and III in glassy toluene solutions are very similar to those in frozen AN solutions.

Luminescence Lifetimes. In each case studied, the emission decays observed for the three clusters as solids proved to be single exponentials with lifetimes independent of the monitoring wavelength (Table II). The same was true for 77 K frozen acetonitrile solutions prepared with concentration of ~10^{-3} M (Table III). For solutions prepared with $[Cu_4X_4(dpmp)_4] \leq 10^{-4}$ M, the luminescence decays tended to be nonexponential, but analysis according to an assumed double exponential showed the longer components displayed lifetimes comparable to those at the higher concentrations; e.g., $\tau_1 = 15.6$ μs (preexponential weighting factor $A_1 \sim 1$) and $\tau_2 = 3.6$ μs ($A_2 \sim 1$) for [I] = 1.26×10^{-4} M.

Discussion

The three compounds of interest here (I, II and III) have been shown to have "cubane"-type $Cu_4X_4L_4$ tetramers with isomorphous and isostructural crystal lattices. The Cu_4X_4 cores consist of a Cu_4 tetrahedron embedded within a somewhat larger X_4 tetrahedron so that the Cu and halide atoms lie at alternate corners of the distorted "cubane" while the ligands bound to each Cu form another, much larger, tetrahedron (Figure 1). The average Cu–Cu distances in the Cu_4 tetrahedra are very close, the respective values being 2.89 ± 0.01, 2.88 ± 0.01 and 2.92 ± 0.08 Å for the chloride, bromide and iodide clusters.[13] The principal structural differences result from the increasing sizes of the halides leading to larger X_4 tetrahedra and to some extension of the Cu–N bond lengths (1.995, 2.024 and 2.065 Å, respectively) owing to steric crowding between the bulky organic ligand and the halides. In all other respects the clusters are structurally very analogous.

Table IV. Intramolecular Cu–Cu Distances (d_{Cu-Cu}) of $Cu_4X_4L_4$ Clusters

cluster	d_{Cu-Cu} (Å)	cluster	d_{Cu-Cu} (Å)
$Cu_4I_4(pip)_4$[a]	2.63–2.67	$Cu_4I_4(dpmp)_4$[b]	2.87–3.01
$Cu_4I_4(py)_4$[c]	2.63–2.79	$Cu_4Br_4(dpmp)_4$[b]	2.87–2.89
$Cu_4Cl_4(Et_3N)_4$[d]	3.07	$Cu_4Cl_4(dpmp)_4$[b]	2.88–2.90

[a] Schramm, V. *Inorg. Chem.* **1978**, *17*, 714–718. [b] Reference 13. [c] Raston, C. L.; White, A. H. *J. Chem. Soc., Dalton Trans.* **1976**, 2153–2156. [d] Dyason, J. C.; Healy, P. C.; Engelhardt, L. M.; Pakawatchai, C.; Patrick, V. A.; Raston, C. L.; White, A. H. *J. Chem. Soc., Dalton Trans.* **1985**, 831–838.

The following observations must be considered in assigning the excited states responsible for the emissions observed for the $Cu_4X_4(dpmp)_4$ complexes: (1) For each the optical spectrum in acetonitrile solution shows absorbances at wavelengths longer than those bands which can be assigned to the π–π^* absorptions of the aromatic ligand or to the halide. These absorbances follow linear Beer's law behavior over the concentration range 10^{-4} to 6×10^{-3} M thus indicate that the species responsible, presumably the $Cu_4X_4(dpmp)_4$ clusters, remain intact in solution. (2) In the same wavelength region (~370 nm) the diffuse reflectance spectra of the solids display bands which match well with the λ_{max}^{ex} observed in the excitation spectra of these materials as well as of AN solutions of the same. (3) At 77 K, the emission spectrum of each $Cu_4X_4(dpmp)_4$ (either as a solid or in frozen AN solution) displays a visible region band, the energy order following the sequence I > II > III. These bands are slightly red-shifted in frozen solution relative to the solids. At 298 K, the emission bands for solid $Cu_4X_4(dpmp)_4$ are slightly blue-shifted relative to the 77 K spectra while no emission was observed from the solutions. (4) There is a substantial Stokes shift (6400–7800 cm^{-1} for the solids at 77 K) between the respective excitation and emission maxima. (5) Luminescence lifetimes are relatively long (>10 μs at 77 K, >0.5 μs at 298 K) implying that the transitions involved are forbidden, most likely spin-forbidden emissions from triplet ES. (6) As solids, the $Cu_4X_4(dpmp)_4$ clusters show a low energy shoulder in the emission spectrum at higher temperature which has a lifetime identical to that of the principal emission band.

A survey of possible excited states relevant to the emission spectra of these dpmp clusters would have to include ligand centered π–π^* state(s), Cu_4X_4 cluster centered state(s) (the result of either XMCT or d → s transitions or a mixture of the two), MLCT states and/or halide to ligand charge transfer (XLCT) states. Of these, the π–π^* ES is unlikely to be the emitting state given that phosphorescence spectra of pyridinium salts display λ_{max}^{em} values (~400 nm) at much higher energy than seen for $Cu_4X_4(dpmp)_4$.[17]

As noted in the Introduction, a variety of arguments led to the conclusion that the intense LE band in the emission spectrum of $Cu_4I_4(py)_4$ is from a CC excited state of mixed XMCT/d–s character while the HE band (much less intense at room temperature) is of XLCT character. These were based in part on ab initio calculations which concluded that, for A as well as for the hypothetical cluster $Cu_4I_4(NH_3)_4$, the highest occupied molecular orbitals in the ground state are not metal centered but are largely iodide p-orbitals (>80%) in character.[1c,2,3,9] Occupied MO's which have substantial metal character were at much lower energy. Examples of XLCT ES's are well documented in a recent

(17) (a) Motten, A. G.; Kwiram, A. L. *J. Chem. Phys.* **1981**, *75*, 2608–2615. (b) Motten, A. G.; Kwiram, A. L. *Chem. Phys. Lett.* **1977**, *45*, 217–220.

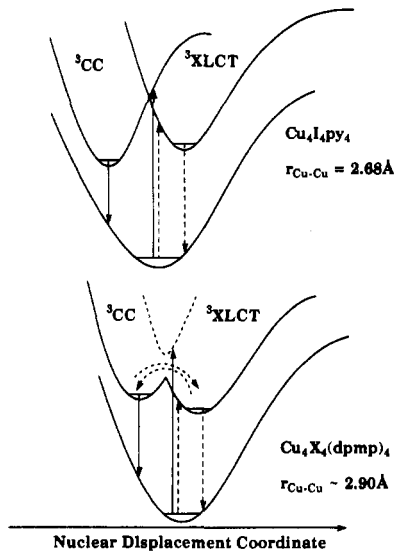

Figure 7. Proposed model for potential energy surfaces for XLCT and CC ES's: top, $Cu_4I_4(py)_4$; bottom, $Cu_4X_4(dpmp)_4$.

review,[18] which also draws the analogy between such metal complexes and the CT transitions seen in pyridinium halide ion pairs, $[RNC_5H_5]^+X^-$.[19] The mixed ligand $Cu_4X_4L_4$ clusters fit this analogy well. At least for A, MLCT states would appear to be higher in energy than either the CC or XLCT states.

In contrast, the relative insensitivity of the 77 K emission and excitation spectra of the three $Cu_4X_4(dpmp)_4$ clusters to the identity of X would appear to argue against an assignment of the emitting ES as having XLCT or XMCT character. Furthermore, one might expect the energy order of such states to be I < Br < Cl, since this is the order of the halide anion gas phase ionization energies[20] and of the halide ion optical electronegativities.[21] However, the opposite energy order was observed for the emission maxima under these conditions. Thus, assignment of the lowest energy, i.e., emitting, ES as a MLCT or metal centered d–s state might appear more consistent, although both assignments would be in contradiction to the results of the ab initio calculations for the related iodide clusters (see below).

Previous examination of the photophysical properties of a series of cuprous chloride clusters $Cu_4Cl_4L_4$ have led to the conclusion that the observed emission bands are not from d–s excited states. The key point is that, while emission was observed with several pyridine derivatives $Cu_4Cl_4(py\text{-}R)_4$ (with the λ_{max}^{em} responsive to the nature of the pyridine substituents R), none was seen when L is a saturated ligand such as Et_3N. Similarly, the spectroscopic features of the cuprous iodide cluster $Cu_4I_4(dpmp)_4$ parallel those described for the HE bands of the dual emitting $Cu_4I_4(py\text{-}R)_4$ clusters[2] which are seen only when L has π-unsaturated acceptor orbitals. The λ_{max}^{em} of I and III are comparable to their pyridine analogues, i.e., 438 and 446 nm for $Cu_4I_4L_4$ with L = py and dpmp and 519 and 505 nm for $Cu_4Cl_4L_4$ with L = py and dpmp, respectively, in the solid state at 77 K.[2,3] The full bandwidths at half maxima ($\Delta\nu_{1/2}$) of $Cu_4X_4(dpmp)_4$ clusters (~3400 cm^{-1}) at 77 K are similar to those of the HE emission bands of $Cu_4I_4(py\text{-}R)_4$ (3100 cm^{-1} in solids to 3800 cm^{-1} in solutions)[2] and to those of the single emission band of $Cu_4Cl_4(py)_4$ (3400 cm^{-1}).[3] Furthermore, the energy differences between the excitation and emission maxima, (6.3–7.4) × 10^3 cm^{-1}, are comparable to those observed for the HE band in the $Cu_4I_4(py\text{-}x)_4$ clusters and to the emission band seen for $Cu_4Cl_4(py)_4$. By comparison, not only is the energy of the LE band found for the other $Cu_4I_4(py\text{-}R)_4$ clusters much lower than seen for $Cu_4I_4(dpmp)_4$, the Stokes shift is much larger (>10 000 cm^{-1}) and the band significantly narrower (~2000 cm^{-1}) under comparable conditions. These observations support the conclusion that the single bands observed in the 77 K emission spectra of I, II and III, like the HE band of A and the single emission seen for $Cu_4Cl_4(py)_4$, involve ligand π-orbitals, i.e., are either MLCT or XLCT. Therefore, in analogy to the assignments of the HE emission from A and the emission from $Cu_4Cl_4(py)_4$, the ES responsible for these emission bands in the dpmp cluster are assigned as being ^{3}XLCT in character.

How can one justify this assignment in the context of the emission energy order I > II > III which seems counterintuitive given the optical electronegativity order $I^- < Br^- < Cl^-$? The explanation can be drawn from the ionicity of the Cu_4X_4 cores.[3] The ionicity of cuprous halides increase in sequence CuI < CuBr < CuCl, and the increasing ionicity of the clusters $Cu_4I_4L_4$ < $Cu_4Br_4L_4$ < $Cu_4Cl_4L_4$ is suggested also by ab initio calculations.[9] Greater anionicity leads to higher energy halide orbitals as also does the effect of the higher covalency in the Cu_4X_4 cores of the heavier halides.[22] These opposing effects on the HOMO energies tend to balance each other and to cancel the expected impact of differing electronegativities.[23]

It is notable that, regardless of the precise assignment of the emission band seen in the 77 K emission spectrum for the cuprous iodide cluster I, this band is clearly analogous to the HE band seen in the emission spectrum of A rather than the much more predominant lower energy band given a CC assignment for the latter species. This would appear to be consistent with the proposal[7] that this type of emission requires a GS structure with Cu–Cu distances less than 2.8 Å. Notably, the d_{Cu-Cu} for I, II and III (~2.90 Å) all lie somewhat outside this proposed limit. However, although no LE emission was seen in the 77 K spectra of these structurally very similar complexes, all three display emissions at longer wavelengths characteristic of CC emissions when the spectra were recorded at temperatures above 200 K (Figure 5). Since the extent of this LE emission is temperature dependent with the apparent activation energies ~1000 cm^{-1}, and the lifetimes at both wavelengths are identical, the logical explanation is that the two states responsible for these two emission bands are in thermal equilibrium and that the ES leading to the lower energy emission is actually at a higher energy on the excited state manifold than is the ES leading to the major emission band. The seeming incongruity of this switch can easily be attributed to the CC state being much more distorted than is the XLCT ES relative to the GS.

Figure 7 proposes a qualitative model for the emitting excited states of the clusters $Cu_4I_4(py)_4$ and $Cu_4X_4(dpmp)_4$. For A the CC state leads not only to the lower energy emission band, but because it gives the longer lived and most intense emission at room temperature it has also been argued to be the lower energy ES. In contrast, the CC ES in the dpmp clusters such as I and II has been shown by temperature effects to be about 1000 cm^{-1} higher in energy than the XLCT ES which is responsible for the principal emission band at all T and is the only emission seen at low T. The poor coupling in the pyridine complex between these two ES is attributed to high barrier height at the curve crossing, so that once the molecule is prepared in either state, the internal

(18) Vogler, A.; Kunkely, H. *Comments Inorg. Chem.* **1990**, *9*, 201–220.
(19) Kosower, E. M. *Prog. Phys. Org. Chem.* **1965**, *3*, 81–163.
(20) Rosenstock, H. M.; Sims, D.; Schroyer, S. S.; Webb, W. J. *Ion Energetic Measurements. Part 1, 1971–1973*; National Standard Reference Data System; NBS: Washington, DC, Sept 1980.
(21) Ferraudi, G. J. *Elements of Inorganic Photochemistry*; John Wiley & Sons, Inc.: New York, 1988; Chapter 5.
(22) Teo, B.-K.; Calabrese, J. C. *Inorg. Chem.* **1976**, *15*, 2474–2486.
(23) From +1.5 to −1.5 V vs Ag/AgCl, only one cyclic wave was observed at positive potential for II and III, $E_{1/2}$ = 0.58 and 0.57 V (peak separations ΔE_p = 87 and 90 mV), respectively. The cyclic voltammogram of I was complicated by iodide oxidation especially with the Pt-disk working electrode. The first positive scan with a clean Pt-disk electrode showed an irreversible anodic peak at E_{pa} = 0.44 V followed by one oxidation wave at $E_{1/2}$ = 0.69 V (ΔE_p = 100 mV). Similar results were observed with a Au-disk working electrode. Under the same electrochemical conditions, the CV for free KI showed similar results with peaks at $E_{1/2}$ = 0.22 V (ΔE_p = 155 mV) and 0.68 V (ΔE_p = 84 mV). This result suggests that the $E_{1/2}$ of I may be higher than that of II and III.

conversion rate is slow relative to other photophysical processes. A much lower barrier height is proposed for the dpmp complexes so that the two states are in thermal equilibrium thus have the same lifetimes under conditions where both emissions are evident.

In what manner can one rationalize these differences? It is clear that the Cu–Cu internuclear distances in the GS have major influence on the emission properties in the context that the CC emissions are certainly less likely to be observed for those complexes having the longer d_{Cu-Cu}. For example, no emission has been seen for $Cu_4Cl_4(Et_3N)_4$ (d_{Cu-Cu} = 3.07 Å), strong CC emission is seen for A and B (d_{Cu-Cu} = 2.65 and 2.68 Å, respectively), and a weak temperature dependent CC emission is seen for solid I and II ($d_{Cu-Cu} \sim 2.90$ Å). In contrast, it would appear (on a limited basis set for comparison) that XLCT emissions are dependent on the nature of the ligand L but are not affected by the Cu–Cu internuclear distances.

Interaction between the filled d-orbitals is Cu–Cu repulsive, while interaction between the Cu s-orbitals is Cu–Cu bonding. In the CC ES, electron density has moved from copper d- to copper s-orbitals, thus the energy of this ES and the shape of its potential surface depends strongly on the extent of Cu–Cu interaction. The shorter d_{Cu-Cu} values would hence lead to greater overlap between relevant orbitals and larger metal–metal interaction. The packing of the large iodide spheres with the smaller Cu(I) spheres in the $Cu_4I_4L_4$ clusters A and B with relatively small ligands L forces the copper atoms into a Cu_4 tetrahedron with short d_{Cu-Cu} values to give greater orbital overlap and a lowest energy, highly distorted CC ES. In contrast, the packing with the smaller chlorides in the chloride clusters C and $Cu_4Cl_4(py)_4$, gives a larger Cu_4 tetrahedron, and as a result no CC emission is seen for either of these clusters. The three dpmp clusters may differ from these other examples in the context that the packing in the Cu_4X_4 core appears to be dominated by the steric bulk of the 2-(diphenylmethyl)pyridine ligand which (fortuitously) holds the d_{Cu-Cu} for all three at ~2.9 Å, a value at which the Cu–Cu interactions are apparently strong enough to give a moderately distorted CC ES whose energy is above but near that of the lowest energy XLCT state from which the emission is principally observed.

Conclusions

The photophysical properties of the copper(I) halide clusters $Cu_4X_4(dpmp)_4$ have been interpreted to derive from the presence of two ES of different origins but close energies. The higher energy, more intense emission is thought to originate from the lowest lying ES, which is assigned as XLCT by analogy with the HE emission of $Cu_4I_4(py)_4$. The lower energy thermally activated emission band is attributed, on the other hand, to a CC ES of slightly higher energy than the XLCT. The activation barrier for the communication between the two excited states is lower in these compounds than it is in $Cu_4I_4(py)_4$. The relative insensitivity of the emission and excitation energy to the nature of the halide is tentatively explained as the result of the ionicity trend having an effect equal and opposite to the electronegativity trend.

Listing of Abbrevations. The following abbreviations were used in the text: A = $Cu_4I_4(py)_4$; AN = CH_3CN; B = $Cu_4I_4(pip)_4$; C = $Cu_4Cl_4(Et_3N)_4$; CC = cluster centered; dpmp = 2-(diphenylmethyl)pyridine; DR = diffuse reflectance; ES = excited state(s); Et_3N = triethylamine; GS = ground state; HE = higher energy; HOMO = highest occupied molecular orbital; I = $Cu_4I_4(dpmp)_4$; II = $Cu_4Br_4(dpmp)_4$; III = $Cu_4Cl_4(dpmp)_4$; L = ligand; LE = lower energy; MC = metal centered; MLCT = metal-to-ligand charge transfer; pip = piperidine; py = pyridine; X = halide; XLCT = halide-to-ligand charge transfer; XMCT = halide-to-metal charge transfer.

Acknowledgment. This research was supported by the U.S. National Science Foundation (Grants CHE-8722561 and CHE-9024845). We thank Professors G. Stucky and W. Kaska for allowing access to the diffuse reflectance spectrometer and electrochemical instruments, respectively. We also thank Dr. N. L. Keder for aid in X-ray powder diffraction studies.